The Journal of Engineering

WILEY

IET The Institution of Engineering and Technology

ORIGINAL RESEARCH OPEN ACCESS

Structured Singular Value Control With General Two-Degree-of-Freedom Feedback Loop Factorisation for Single-Input Single-Output Systems

Marek Dlapa

Faculty of Applied Informatics, Tomas Bata University in Zlin, Zlin, Czech Republic

Correspondence: Marek Dlapa (dlapa@utb.cz)

Received: 12 February 2025 | **Revised:** 3 July 2025 | **Accepted:** 20 July 2025

Funding: This work was supported by the European Regional Development Fund under the project CEBIA-Tech Instrumentation No. CZ.1.05/2.1.00/19.0376 and by the Ministry of Education, Youth and Sports of the Czech Republic within the National Sustainability Programme project No. LO1303 (MSMT-7778/2014).

ABSTRACT

General two-degree-of-freedom feedback loop factorisation for single-input single-output systems applied to oscillating plants with time delay, periodic changes of the controlled plant parameters and astatism using the D-K iteration and algebraic approach is described in this paper. The algebraic approach combines the structured singular value, algebraic theory and algorithm of global optimisation solving remaining issues in structured singular value framework. The algorithm for global optimisation can be alternated with direct search methods such as Nelder-Mead simplex method giving solutions for problems with one local extreme for final tune-up optimisation. As a global optimisation method, Differential Migration is used proving to be reliable in solving this type of problems. The D-K iteration is used as a reference method representing standard procedure for deriving optimal controller in the structured singular value theory. The results obtained from the D-K iteration are compared with the algebraic approach.

1 | Introduction

Robust control of systems with uncertain parameters is subject to research for decades. Rarely, the parameters of the controlled plant are known exactly and, often, the parameters of the physical objects vary in time, that is, the plants are not time-invariant. In this paper, the problem of uncertain time delay and periodic changes of the controlled plant parameters with and without astatism is solved using the D-K iteration and algebraic approach with subsequent factorisation of the simple feedback loop controller to two-degree-of-freedom feedback loop controller. The essential tool is the structured singular value denoted μ (see [1]) giving a measure of robust performance and stability. The algebraic approach (see [2, 3] and [4]) and evolutionary algorithm Differential Migration (see [5]) are used treating the problem of multimodality of the cost function and impossibility of deriving controller for performance weights with poles on the imaginary axis. This implies that the final controller provides zero steady-state error being impossible in the scope of the standard tools using DGKF formulae for obtaining H_∞ (sub)optimal controllers or other methods such as linear matrix inequality (LMI) approach leading to numerical problems in most of real world cases (see [6, 7] and [8]). The algebraic approach overcomes some difficulties connected with the D-K iteration, namely the fact that it does not guarantee convergence to a global or even local minimum (see [9]). Controllers obtained via the algebraic approach can have simpler structure due to the fact that there is no need of scaling matrices absorbance into generalised plant, hence, there is no need of further simplification causing deterioration of the frequency properties of the resulting controller. Moreover, the controller structure can be chosen in advance being not possible in the scope of currently used methods.

Due to multimodality of the cost function, evolutionary algorithm is used providing solution for global optimisation. Evolutionary algorithms belong to the new branches of artificial intelligence (see [10, 11] and [12]) treating the problems being not solvable using traditional optimisation tools. In this paper, a new evolutionary algorithm—Differential Migration—is used having some favourable properties compared to the existing ones, namely the fact that lower computational time is needed for obtaining a suitable solution.

In the proposed method, pole placement for the nominal feedback loop is derived via solving the Diophantine equation in the ring of Hurwitz-stable and proper rational functions (denoted $\mathcal{S}$). The structured singular value evaluates the robust stability and performance of the controller.

Two-degree-of-freedom structure with factorisation of simple feedback controller to feed-forward, feedback and compensator part applicable to two-degree-of-freedom feedback interconnection (1DOF and 2DOF, see [13]) is derived for both D-K iteration and the algebraic μ-synthesis using factorisation of the simple feedback loop controller resulting in general procedure applicable to both controller derivation methods.

For comparison reasons, the controllers obtained from the D-K iteration (see [14]) demonstrate the differences between the standard and proposed method. The overall performance is verified by simulations of step response for maximum values of time delays in nominal and perturbed plant as well as the plant perturbed by the periodic changes of its parameters and maximum time delay in simple feedback loop and two-degree-of-freedom interconnection.

The following notation is used: $\|\cdot\|$ denotes H_∞ norm, $\overline{\sigma}(\cdot)$ is maximum singular value, $\mathbb{N}$, $\mathbb{R}$, $\mathbb{R}^{n\times m}$ and $\mathbb{C}$, $\mathbb{C}^{n\times m}$ $(n, m \in \mathbb{N})$ are natural numbers, real numbers and matrices and complex numbers and matrices, respectively, and $\mathbf{I}_n$ is the unit matrix of dimension n.

2 | Preliminaries

Define $\mathbf{\Delta}$ as a set of block diagonal matrices

$$\begin{aligned}\mathbf{\Delta} \equiv \{diag\,[&\delta_1^C\mathbf{I}_{r_1},\dots,\delta_S^C\mathbf{I}_{r_S},\delta_1^R\mathbf{I}_{c_1},\dots,\delta_T^R\mathbf{I}_{c_T},\\ &\Delta_1^C,\dots,\Delta_F^C,\Delta_1^R,\dots,\Delta_K^R]\ :\\ &\delta_s^C\in\mathbb{C}, s=1\dots S, \delta_t^R\in\mathbb{R}, t=1\dots T,\\ &\Delta_f^C\in\mathbb{C}^{m_f^1\times m_f^2}, f=1\dots F, \Delta_k^R\in\mathbb{R}^{n_k^1\times n_k^2}, k=1\dots K,\\ &r_1\dots r_S, c_1\dots c_T\in\mathbb{N},\\ &m_1^1\dots m_F^1, m_1^2\dots m_F^2, n_1^1\dots n_K^1, n_1^2\dots n_k^2\in\mathbb{N},\\ &s,t,f,k,S,T,F,K\in\mathbb{N}\}\end{aligned} \tag{1}$$

For consistency among all the dimensions, the following condition must be held

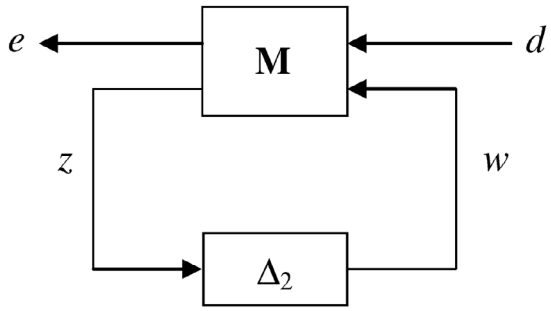

FIGURE 1 | LFT interconnection.

$$\begin{aligned}\sum_{s=1}^{S} r_s + \sum_{t=1}^{T} c_t + \sum_{f=1}^{F} m_f^1 + \sum_{k=1}^{K} n_k^1 = n\\ \sum_{s=1}^{S} r_s + \sum_{t=1}^{T} c_t + \sum_{f=1}^{F} m_f^2 + \sum_{k=1}^{K} n_k^2 = m\end{aligned} \tag{2}$$

Definition 1. For $\mathbf{M}\in\mathbb{C}^{n\times m}$ is $\mu_{\mathbf{\Delta}}(\mathbf{M})$ defined as

$$\mu_{\mathbf{\Delta}}(\mathbf{M}) \equiv \frac{1}{\min\{\overline{\sigma}(\Delta)\ :\ \Delta\in\mathbf{\Delta}, \det(\mathbf{I}-\mathbf{M}\Delta)=0\}} \tag{3}$$

If no such $\Delta\in\mathbf{\Delta}$ exists making $\mathbf{I}-\mathbf{M}\Delta$ singular, then $\mu_{\mathbf{\Delta}}(\mathbf{M})=0$.

Consider a complex matrix $\mathbf{M}$ partitioned as

$$\mathbf{M} = \begin{bmatrix}\mathbf{M}_{11} & \mathbf{M}_{12}\\ \mathbf{M}_{21} & \mathbf{M}_{22}\end{bmatrix} \tag{4}$$

and suppose there is a defined block structure Δ_2 which is compatible in size with $\mathbf{M}_{22}$ (for any $\Delta_2\in\mathbf{\Delta_2}$, $\mathbf{\Delta_2}\subset\mathbf{\Delta}$, $\mathbf{M}_{22}\Delta_2$ is square). For $\Delta_2\in\mathbf{\Delta_2}$, consider the following loop equations

$$\begin{aligned}e &= \mathbf{M}_{11}d + \mathbf{M}_{12}w\\ z &= \mathbf{M}_{21}d + \mathbf{M}_{22}w\\ w &= \Delta_2 z\end{aligned} \tag{5}$$

If the inverse to $\mathbf{I}-\mathbf{M}_{22}\Delta_2$ exists, then e and d must satisfy $e=\mathbf{F}_L(\mathbf{M},\Delta_2)d$, where

$$\mathbf{F}_L(\mathbf{M},\Delta_2) = \mathbf{M}_{11} + \mathbf{M}_{12}\Delta_2(\mathbf{I}-\mathbf{M}_{22}\Delta_2)^{-1}\mathbf{M}_{21} \tag{6}$$

is a linear fractional transformation on $\mathbf{M}$ by Δ_2 and in a feedback diagram appears as the loop in Figure 1.

The subscript L on $\mathbf{F}_L$ pertains to the *lower* loop of $\mathbf{M}$ and is closed by Δ_2. An analogous formula describes $\mathbf{F}_L(\mathbf{M},\Delta_2)$ which is the resulting matrix obtained by closing the *upper* loop of $\mathbf{M}$ with a matrix $\Delta_1\in\mathbf{\Delta_1}$, $\mathbf{\Delta_1}\subset\mathbf{\Delta}$.

Theorem 1. *Let $\beta>0$. For all $\Delta_2\in\mathbf{\Delta_2}$ with $|\overline{\sigma}(\Delta_2)|<\frac{1}{\beta}$, the loop shown in Figure 1 is well-posed, internally stable, and $\|\mathbf{F}_L(\mathbf{M},\Delta_2)\|_\infty\le\beta$ if and only if*

$$\sup_{\omega\in\mathbb{R}}\mu_{\mathbf{\Delta}}[\mathbf{M}(j\omega)]\le\beta \tag{7}$$

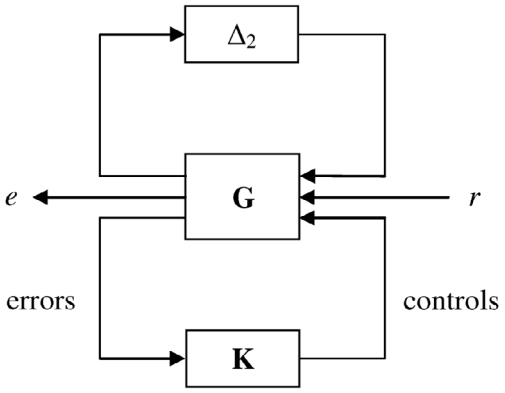

FIGURE 2 | Closed loop interconnection.

Proof. Proof is the same as in [15] and [1] except for the fact that perturbations are complex matrices which simplifies the proof and complies with the definition of μ-function. □

3 | Algebraic μ-Synthesis

The algebraic μ-synthesis is applicable to any control problem transformable to the loop in Figure 2 where **G** denotes the generalised plant, **K** is the controller, Δ_{del} is the perturbation matrix, r is the reference and e is the output.

The MIMO system with l inputs and l outputs can be decoupled into l identical SISO plants. In terms of continuous-time transfer functions, the nominal model is defined as:

$$\mathbf{P}_{nom}(s) \equiv \begin{bmatrix} \mathbf{P}_{11}(s) & \cdots & \mathbf{P}_{1l}(s) \\ \vdots & \ddots & \vdots \\ \mathbf{P}_{l1}(s) & \cdots & \mathbf{P}_{ll}(s) \end{bmatrix} \tag{8}$$

For decoupling the nominal plant $\mathbf{P}_{nom}(s)$ [$\mathbf{P}_{nom}(s)$ invertible], it is satisfactory to define the controller as

$$\mathbf{K}(s) = K(s)\mathbf{I}_l \frac{1}{P_{xy}(s)} adj[\mathbf{P}_{nom}(s)] \tag{9}$$

where P_{xy} is an element of $adj[\mathbf{P}_{nom}(s)] = \det[\mathbf{P}_{nom}(s)] \cdot [\mathbf{P}_{nom}(s)]^{-1}$ with the highest degree of numerator $\{adj[\mathbf{P}_{nom}(s)]$ denotes adjugate matrix of $\mathbf{P}_{nom}\}$. The definition of decoupling matrix prevents the controller from cancelling any unstable poles or zeros so that internal stability of the nominal feedback loop is held. The MIMO problem is reduced to finding a controller $K(s)$ tuned by the poles of the nominal feedback loop with the plant

$$\begin{aligned} \mathbf{P}_{dec}(s) &= \frac{1}{P_{xy}(s)} \det[\mathbf{P}_{nom}(s)] \mathbf{P}_{nom}(s)^{-1} \mathbf{P}_{nom}(s) \\ \mathbf{P}_{dec}(s) &= \frac{1}{P_{xy}(s)} \det[\mathbf{P}_{nom}(s)] \mathbf{I}_l \end{aligned} \tag{10}$$

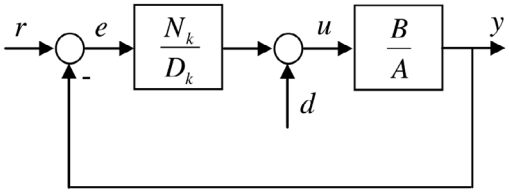

FIGURE 3 | Nominal feedback loop.

Equation (10) follows the nominal plant transfer function used in algebraic approach controller derivation:

$$P_{dec}(s) = \frac{1}{P_{xy}(s)} \det[\mathbf{P}_{nom}(s)] \tag{11}$$

Transfer function P_{dec} can be approximated by a system P^*_{dec} with lower order than P_{dec}

$$P^*_{dec}(s) = \frac{b(s)}{a(s)} \tag{12}$$

and rewritten in terms of its coefficients and transformed to the elements of $\mathcal{S}$

$$P^*_{dec}(s) = \frac{\frac{b_n s^n + b_{n-1} s^{n-1} + \cdots + b_1 s + b_0}{(\alpha_1 + s)(\alpha_2 + s) \cdot \ldots \cdot (\alpha_n + s)}}{\frac{a_n s^n + a_{n-1} s^{n-1} + \cdots + a_1 s + a_0}{(\alpha_1 + s)(\alpha_2 + s) \cdot \ldots \cdot (\alpha_n + s)}} \tag{13}$$

The controller $K = N_K/D_K$ is obtained by solving the Diophantine equation

$$AD_K + BN_K = 1 \tag{14}$$

with $A, B, D_K, N_K \in \mathcal{S}$. Equation (14) is the Bezout identity. All feedback controllers N_K/D_K are given by Youla parametrisation

$$K = \frac{N_K}{D_K} = \frac{N_{K_0} - AT}{D_{K_0} + BT}, N_{K_0}, D_{K_0} \in \mathcal{S} \tag{15}$$

where $N_{K_0}, D_{K_0} \in \mathcal{S}$ are particular solutions of (14) and T is an arbitrary element of $\mathcal{S}$.

The controller K satisfying Equation (14) guarantees the BIBO (bounded input bounded output) stability of the feedback loop in Figure 3. The BIBO stability is not necessary condition for theorems related to robust stability and performance but, without loss of generality, simplifies searching the optimal or stabilising tuning parameters α_i with $i = 1, 2, \ldots n + n_1 + n_2$ and arbitrary transfer function $T \in \mathcal{S}$. If the controller or nominal plant has an astatism, then stabilising controller exists even if performance weights with astatism are used implying non-existence of state-space solutions using DGKF formulae (see [6]) due to zero eigenvalues of appropriate Hamiltonian matrices. Such procedure results in zero steady-state error in the feedback loop with the controller obtained as a solution to Equation (14). This technique is neither possible in the scope of the standard μ-synthesis using DGKF formulae, nor using LMI approach (see [7]) leading to numerical problems in most of real-world applications, except algebraic μ-synthesis solving this issue.

The aim of synthesis is to find a controller satisfying the condition (using α_i and t_i as tuning parameters):

$$\sup_{\omega} \mu^{u}_{\Delta}[\mathbf{F}_L(\mathbf{G},\mathbf{K})(j\omega,\alpha_1,\dots,\alpha_{n+n_1+n_2},t_1,\dots,t_{n_2})] \leq 1, \omega \in [0,\infty) \tag{16}$$

where μ^{u}_{Δ} denotes upper bound μ, ω is angular velocity in Fourier transform, $n+n_1+n_2$ is the order of the nominal feedback system, n_1 is the order of particular solution K_0, t_i are arbitrary parameters in $T = \frac{t_{n_2}s^{n_2}+t_{n_2-1}s^{n_2-1}+\cdots+t_1 s+t_0}{(\alpha_{n+n_1+1}+s)(\alpha_{n+n_1+2}+s)\cdot\ldots\cdot(\alpha_{n+n_1+n_2}+s)}$ and μ_{Δ} denotes the structured singular value corresponding to uncertainty set $\mathbf{\Delta}$.

Tuning parameters α_i are positive and constrained to the real axis since parameters of the controller transfer function have to be real and due to the fact that non-real poles cause oscillations of the nominal feedback loop.

The cost function in (16) has many local extremes, hence, local optimisation does not yield a suitable or even stabilising solution. This issue can be overcome via evolutionary optimisation solving the task more or less efficiently.

4 | Modelling of Parametric Uncertainties for Design Using Structured Singular Value

Consider a general set of plants with uncertain numerator and denominator and uncertain time delay:

$$\tilde{\mathbf{P}} \equiv \left\{ \frac{b_n s^n + b_{n-1}s^{n-1}+\cdots+b_1 s+b_0}{a_n s^n + a_{n-1}s^{n-1}+\cdots+a_1 s+a_0} e^{-\tau s} : \begin{array}{c} a_i \in [\overline{a}_i - da_i, \overline{a}_i + da_i], \\ b_i \in [\overline{b}_i - db_i, \overline{b}_i + db_i], \\ \tau \in [0, T_d], i = 0,1,\dots,n \end{array} \right\} \tag{17}$$

This set of plants corresponds to the interconnection in Figure 4 fitting into the linear fractional transformation (LFT) framework. For the perturbations $\delta_{a_i}, \delta_{b_i} \in \mathbb{R}$, $\delta_{del} \in \mathbb{C}$, the following conditions hold

$$|\delta_{a_i}| < 1,\ |\delta_{b_i}| < 1,\ |\delta_{del}| < 1, i = 0,1,\dots,n \tag{18}$$

The weights W_{a_i}, W_{b_i} and W_{del} must satisfy the following inequalities:

$$W_{a_i} = da_i/(\overline{a}_n s^{n-i}), i = 0,1,\dots,n \tag{19}$$

$$W_{b_i} = db_i/(\overline{a}_n s^{n-i}), i = 0,1,\dots,n \tag{20}$$

$$|W_{del}| > |1 - e^{-T_d j\omega}|, \text{for all } \omega \in \mathbb{R} \tag{21}$$

Set of plants (17) corresponding to the interconnection in Figure 4 can be transformed to the interconnections in Figure 5 where the sensitivity function as a performance indicator is included and $\tilde{\mathbf{P}}_{nom}$ with Δ_2 in feedback loop is the open-loop interconnection from Figure 4.

The perturbation matrix Δ_2 is defined as:

$$\Delta_2 \equiv \begin{bmatrix} \Delta_a & 0 & 0 \\ 0 & \Delta_b & 0 \\ 0 & 0 & \delta_{del} \end{bmatrix} \tag{22}$$

$$\Delta_a \equiv \begin{bmatrix} \delta_{a_0} & 0 & \cdots & 0 \\ 0 & \delta_{a_1} & \cdots & 0 \\ \vdots & \vdots & \ddots & \vdots \\ 0 & 0 & \cdots & \delta_{a_n} \end{bmatrix} \tag{23}$$

$$\Delta_b \equiv \begin{bmatrix} \delta_{b_0} & 0 & \cdots & 0 \\ 0 & \delta_{b_1} & \cdots & 0 \\ \vdots & \vdots & \ddots & \vdots \\ 0 & 0 & \cdots & \delta_{b_n} \end{bmatrix} \tag{24}$$

For stability and performance of the feedback loop depicted in Figure 5, Theorem 2 and subsequent Corollary 1 hold:

Theorem 2. *Assume Δ_2 defined by (18), (22), (23), (24), then the loop in Figure 5 is well-posed, internally stable and $\|\mathbf{F}_L[\mathbf{F}_U(\mathbf{G},\Delta_2),K]\|_\infty \leq 1$ if and only if*

$$\sup_{\omega\in\mathbb{R}} \mu_{\tilde{\Delta}}[\mathbf{F}_L(\mathbf{G},\mathbf{K})(j\omega)] \leq 1 \tag{25}$$

with $\tilde{\mathbf{\Delta}} \equiv \left\{ \begin{bmatrix} \delta_1 & 0 \\ 0 & \Delta_2 \end{bmatrix} : |\delta_1| < 1, \delta_1 \in \mathbb{C} \right\}, \tilde{\mathbf{\Delta}} \subset \mathbf{\Delta}.$

Proof. See [4]. □

The set of sensitivity functions $\tilde{\mathbf{S}}$ is defined as the set of transfer functions from the reference signal r to error e in Figure 6:

$$\tilde{\mathbf{S}} \equiv \left\{ \frac{1}{1+PK} : P \in \tilde{\mathbf{P}} \right\} \tag{26}$$

A sufficient condition for the robust stability and performance of the feedback loop in Figure 6 can be formed for the set of sensitivity functions $\tilde{\mathbf{S}}$ and a family of plants (17) as the consequence of Theorem 2.

Corollary 1. *With assumptions (19), (20), (21) and for every $P \in \tilde{\mathbf{P}}$ defined by (17) and (18), the feedback loop in Figure 6 is well-posed, internally stable and $\|SW_1\|_\infty \leq 1$ for every $S \in \tilde{\mathbf{S}}$ if (25) holds.*

Proof. The proof follows from Figure 4, inequalities (25), (18), definitions (19), (20), (21) and Theorem 2. □

5 | Examples of Uncertain Systems with Periodic Changes of Parameters

5.1 | Plant Definitions

Define the following set of plants with uncertain time delay and uncertain coefficients in numerator and denominator and the corresponding weights (t denotes time):

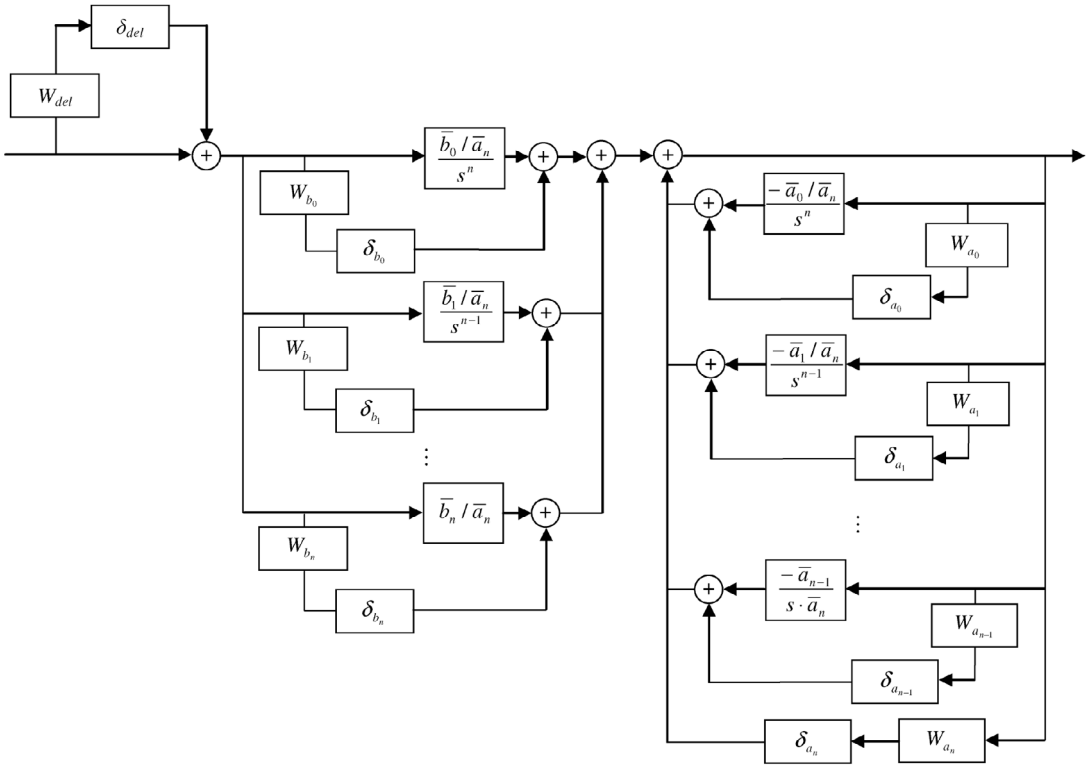

FIGURE 4 | The general parametric uncertainties system interconnection for LFT framework.

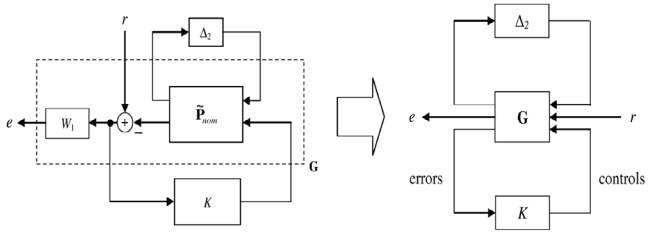

FIGURE 5 | Closed-loop interconnection.

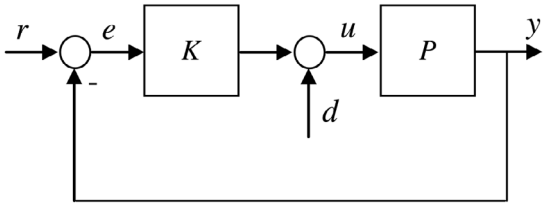

FIGURE 6 | Feedback loop for $P \in \tilde{\mathbf{P}}$.

$$\tilde{\mathbf{P}}_1 \equiv \left\{ \begin{array}{c} \frac{b_{1,0}}{a_{1,3}s^3 + a_{1,2}s^2 + a_{1,1}s + a_{1,0}} \cdot e^{-\tau_1 s} : \\ a_{1,0} = 1, \\ a_{1,1} \in [3-0.3, 3+0.3], a_{1,1} = 3 + 0.3sin(t), \\ a_{1,2} \in [3-0.3, 3+0.3], a_{1,2} = 3 + 0.3sin(t), \\ a_{1,3} = 1, \\ b_{1,0} \in [2-0.2, 2+0.2], b_{1,1} = 2 + 0.2sin(t), \\ \tau_1 \in [0,4] \end{array} \right\} \quad (27)$$

$$W_{a_{1,1}} = 0.3/s^2 \quad (28)$$

$$W_{a_{1,2}} = 0.3/s \quad (29)$$

$$W_{b_{1,0}} = 0.2/s^3 \quad (30)$$

$$|W_{del1}| > |1 - e^{4j\omega}|, \omega \in \mathbb{R} \Rightarrow W_{del1} = \frac{2s}{2s+1} \cdot 2.5 \quad (31)$$

$$W_{1,1}^{A} = \frac{1}{400s^2 + 40s} \quad (32)$$

$$W_{1,1}^{D-K} = \frac{1}{400s^2 + 40s + 0.00001} \quad (33)$$

$$\tilde{\mathbf{P}}_2 \equiv \left\{ \begin{array}{c} \frac{b_{2,0}}{a_{2,4}s^4 + a_{2,3}s^3 + a_{2,2}s^2 + a_{2,1}s} \cdot e^{-\tau_2 s} : \\ a_{2,1} = 1, \\ a_{2,2} \in [3-0.3, 3+0.3], a_{2,2} = 3 + 0.3sin(0.1 \cdot t), \\ a_{2,3} \in [3-0.3, 3+0.3], a_{2,3} = 3 + 0.3sin(0.1 \cdot t), \\ a_{2,4} = 1, \\ b_{2,0} \in [2-0.2, 2+0.2], b_{2,0} = 2 + 0.2sin(0.1 \cdot t), \\ \tau_2 \in [0,4] \end{array} \right\} \quad (34)$$

$$W_{a_{2,2}} = 0.3/s^2 \quad (35)$$

$$W_{a_{2,3}} = 0.3/s \quad (36)$$

$$W_{b_{2,0}} = 0.2/s^4 \quad (37)$$

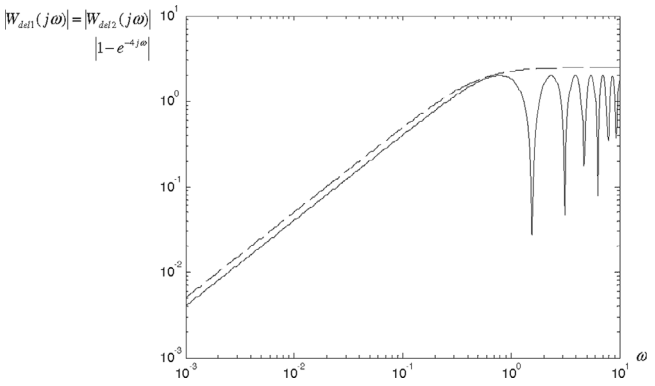

FIGURE 7 | Bode plot of $|W_{del1}| = |W_{del2}|$ (dashed) and $|1 - e^{4j\omega}|$ (full).

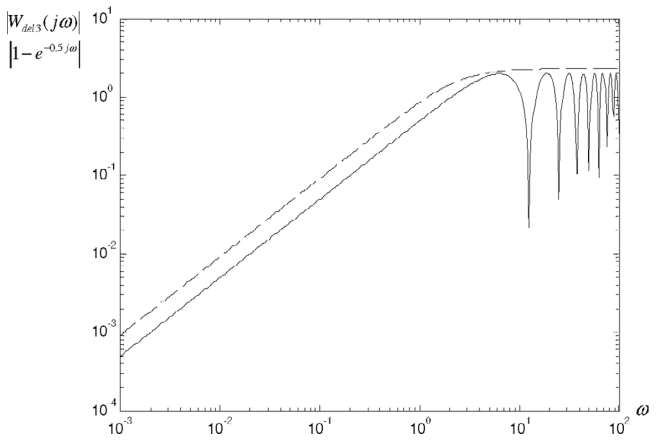

FIGURE 8 | Bode plot of $|W_{del3}|$ (dashed) and $|1 - e^{0.5j\omega}|$ (full).

$$|W_{del2}| > |1 - e^{4j\omega}|, \omega \in \mathbb{R} \Rightarrow W_{del2} = \frac{2s}{2s+1} \cdot 2.5 \tag{38}$$

$$W_{2,1}^{A} = \frac{1}{400s^2 + 40s} \tag{39}$$

$$W_{2,1}^{D-K} = \frac{1}{400s^2 + 40s + 0.00001} \tag{40}$$

$$\tilde{\mathbf{P}}_3 \equiv \left\{ \begin{array}{c} \frac{b_{3,0}}{a_{3,3}s^3 + a_{3,1}s} \cdot e^{-\tau_3 s} : \\ a_{3,1} \in [1-0.2, 1+0.2], a_{3,1} = 1 + 0.2sin(0.1 \cdot t), \\ a_{3,3} = 1, \\ b_{3,0} \in [1-0.2, 1+0.2], b_{3,0} = 1 + 0.2sin(0.1 \cdot t), \\ \tau_3 \in [0, 0.5] \end{array} \right\} \tag{41}$$

$$W_{a_{3,1}} = 0.2/s^2 \tag{42}$$

$$W_{b_{3,0}} = 0.2/s^3 \tag{43}$$

$$|W_{del3}| > |1 - e^{0.5j\omega}|, \omega \in \mathbb{R} \Rightarrow W_{del3} = \frac{2s}{2s+5} \cdot 2.3 \tag{44}$$

$$W_{3,1}^{A} = \frac{0.005}{400s^2 + 40s} \tag{45}$$

$$W_{3,1}^{D-K} = \frac{0.4}{400s^2 + 40s + 0.00001} \tag{46}$$

The bode plots of $|W_{del1}| = |W_{del2}|$, $|1 - e^{4j\omega}|$ and $|W_{del3}|$, $|1 - e^{0.5j\omega}|$ are in Figures 7 and 8, respectively, proving that weights in multiplicative uncertainty satisfy condition (21) being the envelope curve of the right side of inequality (21) with small conservatism. Weights (28), (29), (30), (35), (36), (37), (42) and (43) follow from Equations (19) and (20) with respect to $\tilde{\mathbf{P}}_1, \tilde{\mathbf{P}}_2, \tilde{\mathbf{P}}_3 \subset \mathbf{P}$.

5.2 | Global Optimisation Using Evolutionary Algorithm

In order to overcome multimodality of the cost function (16) evolutionary algorithm Differential Migration is used (DM, [5]) due to shorter time needed for finding global minimum than other algorithms of this type with final tune-up carried out by Nelder–Mead simplex method. Parameters of DM for each controlled plant are in Tables 1–3.

TABLE 1 | DM parameters for the set of plants $\tilde{\mathbf{P}}_1$.

Parameter	Value
Arbitrary polynomial	none
Min. value of α	0
Max. value of α	80
Number of population	30
Jump range	[0.2, 4]
Perturbation constant	0.7
Max. number of migration loops	90
Accepted error	0
Cluster distance	1.3

TABLE 2 | DM parameters for the set of plants $\tilde{\mathbf{P}}_2$.

Parameter	Value
Arbitrary polynomial	none
Min. value of α	0
Max. value of α	2
Number of population	30
Jump range	[0.2, 4]
Perturbation constant	0.7
Max. number of migration loops	150
Accepted error	0
Cluster distance	1.25

Final negated nominal feedback loop poles and arbitrary polynomial obtained via global optimisation and direct search method are:

Set of plants $\tilde{\mathbf{P}}_1$:

$$\begin{array}{c} \alpha_{1,1} = 0.0793; \alpha_{1,2} = 0.6207; \alpha_{1,3} = 1.3709 \\ \alpha_{1,4} = 1.5665; \alpha_{1,5} = 2.0358; \alpha_{1,6} = 30.5718 \end{array} \tag{47}$$

TABLE 3 | DM parameters for the set of plants $\tilde{\mathbf{P}}_3$.

Parameter	Value
Arbitrary polynomial degree	1
Min. value of α	0
Max. value of α	2
Min. value of arbitrary parameters	0
Max. value of arbitrary parameters	10
Number of population	30
Jump range	[0.2, 4]
Perturbation constant	0.7
Max. number of migration loops	60
Accepted error	0
Cluster distance	1.3

Set of plants $\tilde{\mathbf{P}}_2$:

$$\begin{aligned}\alpha_{2,1} &= 0.0482; \alpha_{2,2} = 0.0591; \alpha_{2,3} = 0.5004\\ \alpha_{2,4} &= 1.1622; \alpha_{2,5} = 1.3631; \alpha_{2,6} = 1.4148\\ \alpha_{2,7} &= 1.7386\end{aligned} \tag{48}$$

Set of plants $\tilde{\mathbf{P}}_3$:

$$\begin{aligned}\alpha_{3,1} &= 0.0262; \alpha_{3,2} = 0.9694; \alpha_{3,3} = 1.0708\\ \alpha_{3,4} &= 1.2300; \alpha_{3,5} = 1.2646; \alpha_{3,6} = 1.3130\\ &\text{Arbitrary polynomial: } t(s) = 6.6051s + 4.2687\end{aligned} \tag{49}$$

Final controllers corresponding to negated nominal feedback loop poles and arbitrary polynomial obtained from global optimisation (47)–(49) and controllers obtained via D-K iteration using modified performance weights $W_{1,1}^{D-K}$, $W_{2,1}^{D-K}$ and $W_{3,1}^{D-K}$ are:

Set of plants $\tilde{\mathbf{P}}_1$:

$$K_1^A(s) = \frac{9.442s^3 + 19.1s^2 + 11.82s + 3.29}{s^3 + 33.24s^2 + 82.36s} \tag{50}$$

$$K_1^{D-K}(s) = \frac{(345s^3 + 488s^2 + 272s + 0.767)\cdot 10^{-4}}{s^3 + 0.974s^2 + 0.00292s + 1.02\cdot 10^{-9}} \tag{51}$$

Set of plants $\tilde{\mathbf{P}}_2$:

$$K_2^A(s) = \frac{0.0700s^3 + 0.1805s^2 + 0.1178s + 0.0028}{s^3 + 3.286s^2 + 2.655s + 0.00079} \tag{52}$$

$$K_2^{D-K}(s) = \frac{(-32.8s^4 + 281s^3 + 474s^2 + 118s + 0.856)\cdot 10^{-4}}{s^4 + 0.658s^3 + 2.52s^2 + 0.359s + 1.97\cdot 10^{-7}} \tag{53}$$

Set of plants $\tilde{\mathbf{P}}_3$:

$$K_3^A(s) = \frac{3.4s^6 + 17.2s^5 + 16s^4 - 9.39s^3 - 12.1s^2 - 0.0177s + 0.113}{s^6 + 9.68s^5 + 40s^4 + 86.1s^3 + 92.8s^2 + 43.3s + 5.11} \tag{54}$$

$$K_3^{D-K}(s) = \frac{(-3.304s^3 + 44.34s^2 + 10.56s + 0.103)\cdot 10^{-4}}{s^3 + 0.238s^2 + 0.0271s - 1.46\cdot 10^{-8}} \tag{55}$$

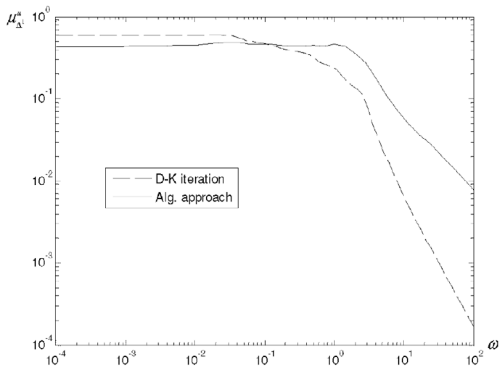

FIGURE 9 | Upper bound μ-plot for the set of plants $\tilde{\mathbf{P}}_1$ with the controllers obtained by the D-K iteration and algebraic approach.

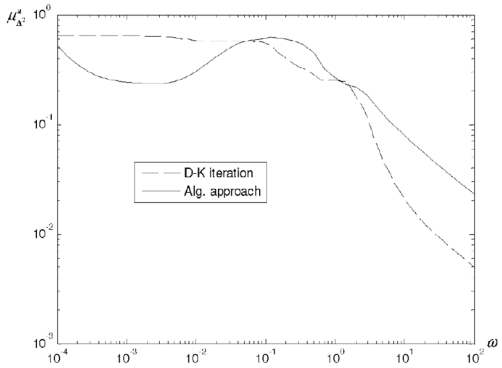

FIGURE 10 | Upper bound μ-plot for the set of plants $\tilde{\mathbf{P}}_2$ with the controllers obtained by the D-K iteration and algebraic approach.

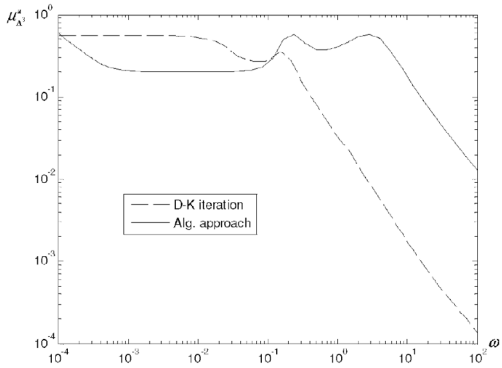

FIGURE 11 | Upper bound μ-plot for the set of plants $\tilde{\mathbf{P}}_3$ with the controllers obtained by the D-K iteration and algebraic approach.

The upper bound μ plots in Figures 9–11 show that both controllers have the supremum of upper bound μ below one and the robust stability and performance conditions in Corollary 1 are satisfied for all controlled plants with maximum values of upper bound μ:

$$\sup_{\omega}\mu_{\Delta^1}^u\left[\mathbf{F}_L\left(\mathbf{G}_1, K_1^A\right)\right] = 0.488, \sup_{\omega}\mu_{\Delta^1}^u\left[\mathbf{F}_L\left(\mathbf{G}_1, K_1^{D-K}\right)\right] = 0.603,$$

$$\sup_{\omega}\mu_{\Delta^2}^u\left[\mathbf{F}_L\left(\mathbf{G}_2, K_2^A\right)\right] = 0.628, \sup_{\omega}\mu_{\Delta^2}^u\left[\mathbf{F}_L\left(\mathbf{G}_2, K_2^{D-K}\right)\right] = 0.644,$$

$$\sup_{\omega}\mu_{\Delta^3}^u\left[\mathbf{F}_L\left(\mathbf{G}_3, K_3^A\right)\right] = 0.596, \sup_{\omega}\mu_{\Delta^3}^u\left[\mathbf{F}_L\left(\mathbf{G}_3, K_3^{D-K}\right)\right] = 0.563$$

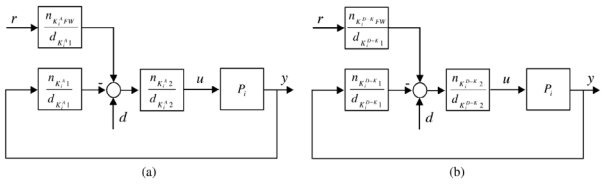

FIGURE 12 | 2DOF feedback loop for $P_i \in \widetilde{\mathrm{P}}_i$ and $i = 1, 2, 3$.

where $\omega \in [0, \infty)$, $\boldsymbol{\Delta}^1$, $\boldsymbol{\Delta}^2$, $\boldsymbol{\Delta}^3 \subset \tilde{\boldsymbol{\Delta}} \subset \boldsymbol{\Delta}$ and $\mathbf{G}_1$, $\mathbf{G}_2$, $\mathbf{G}_3$ correspond to set of plants $\tilde{\mathbf{P}}_1$, $\tilde{\mathbf{P}}_2$, $\tilde{\mathbf{P}}_3$, respectively, fitting into interconnections in Figure 4 and 5.

5.3 | Factorisation for 2DOF Feedback Loop

The controllers for 2DOF feedback loop (Figures 12a,b—algebraic approach and D-K iteration, respectively) have the compensator ($n_{K_i^A 2}$, $d_{K_i^A 2}$, $n_{K_i^{D-K} 2}$, $d_{K_i^{D-K} 2}$) defined as fraction of the factors corresponding to most stable zeros and all unstable poles of K_i^A and K_i^{D-K} and if there are complex conjugate poles or zeros, then the next most stable zero or least stable pole is used, and if there is no such zero and pole, then most stable complex conjugate zeros or least stable complex conjugate poles and two corresponding least stable zeros and most stable poles or complex conjugate zeros or least stable complex conjugate poles are used, so that no single conjugate pole or zero is in numerator or denominator of compensator and equivalently in the feedback part of the controller. If there is no unstable pole of K_i^A and K_i^{D-K}, then most stable zero and least stable pole is used as initial step. Necessary condition for these steps is that no unstable pole of K_i^A and K_i^{D-K} is omitted from $d_{K_i^A 2}$ and $d_{K_i^{D-K} 2}$. The feedback ($n_{K_i^A 1}$, $d_{K_i^A 1}$, $n_{K_i^{D-K} 1}$, $d_{K_i^{D-K} 1}$) and feed-forward part ($n_{K_i^A FW}$, $d_{K_i^A 1}$, $n_{K_i^{D-K} FW}$, $d_{K_i^{D-K} 1}$) are defined by the fraction of the factors corresponding to remaining zeros and poles of K_i^A and K_i^{D-K} with $n_{K_i^A FW} = n_{K_i^A 1,0}$ and $n_{K_i^{D-K} FW} = n_{K_i^{D-K} 1,0}$ ($n_{K_i^A 1,0}$, $n_{K_i^{D-K} 1,0}$ being the coefficients of $n_{K_i^A 1}$ and $n_{K_i^{D-K} 1}$ of zero exponent of s and $i = 1, 2, 3$). In some cases, the least stable zeros can be moved to the compensator instead of the most stable ones.

The necessary condition for the feedback part and compensator is:

$$K_i^A = \frac{n_{K_i^A 1} \cdot n_{K_i^A 2}}{d_{K_i^A 1} \cdot d_{K_i^A 2}}, \; K_i^{D-K} = \frac{n_{K_i^{D-K} 1} \cdot n_{K_i^{D-K} 2}}{d_{K_i^{D-K} 1} \cdot d_{K_i^{D-K} 2}}, \; i = 1, 2, 3 \tag{56}$$

Set of plants $\tilde{\mathbf{P}}_1$:

$$\frac{n_{K_1^A 1}}{d_{K_1^A 1}} = \frac{9.442s^2 + 7.397s + 2.655}{s^2 + 33.24s + 82.36},$$

$$\frac{n_{K_1^A FW}}{d_{K_1^A 1}} = \frac{2.655}{s^2 + 33.24s + 82.36}, \frac{n_{K_1^A 2}}{d_{K_1^A 2}} = \frac{s + 1.239}{s} \tag{57}$$

$$\frac{n_{K_1^{D-K} 1}}{d_{K_1^{D-K} 1}} = \frac{0.0345s^2 + 0.0487s + 0.0271}{s^2 + 0.974s + 0.00292},$$

$$\frac{n_{K_1^{D-K} FW}}{d_{K_1^{D-K} 1}} = \frac{0.0271}{s^2 + 0.974s + 0.00292}, \frac{n_{K_1^{D-K} 2}}{d_{K_1^{D-K} 2}} = \frac{s + 0.00284}{s + 3.51 \cdot 10^{-7}} \tag{58}$$

Set of plants $\tilde{\mathbf{P}}_2$:

$$\frac{n_{K_2^A 1}}{d_{K_2^A 1}} = \frac{0.06957s^2 + 0.08082s + 0.001938}{s^2 + 3.286s + 2.654},$$

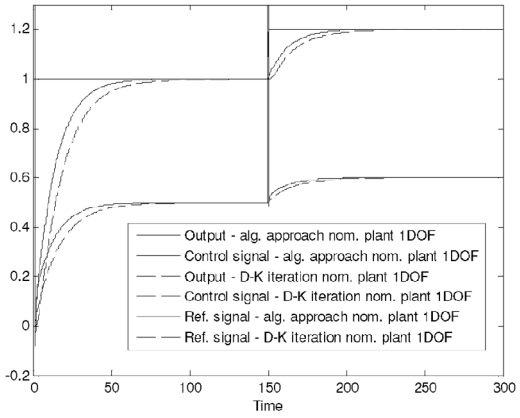

FIGURE 13 | Simulation for simple feedback loop and nominal plant of the set of plants $\tilde{\mathbf{P}}_1$.

$$\frac{n_{K_2^A FW}}{d_{K_2^A 1}} = \frac{0.001938}{s^2 + 3.286s + 2.654}, \frac{n_{K_2^A 2}}{d_{K_2^A 2}} = \frac{s + 1.433}{s + 0.0002988} \tag{59}$$

$$\frac{n_{K_2^{D-K} 1}}{d_{K_2^{D-K} 1}} = \frac{-32.75s^3 + 319.1s^2 + 99.48s + 0.7288}{s^3 + 0.6583s^2 + 2.522s + 0.3587} \cdot 10^{-4},$$

$$\frac{n_{K_2^{D-K} FW}}{d_{K_2^{D-K} 1}} = \frac{7.288 \cdot 10^{-5}}{s^3 + 0.6583s^2 + 2.522s + 0.3587},$$

$$\frac{n_{K_2^{D-K} 2}}{d_{K_2^{D-K} 2}} = \frac{s + 1.175}{s + 5.486 \cdot 10^{-7}} \tag{60}$$

Set of plants $\tilde{\mathbf{P}}_3$:

$$\frac{n_{K_3^A 1}}{d_{K_3^A 1}} = \frac{3.4s^5 + 4.92s^4 - 1.68s^3 - 3.35s^2 - 0.0137s + 0.0315}{s^5 + 9.51s^4 + 38.35s^3 + 79.46s^2 + 79.11s + 29.67},$$

$$\frac{n_{K_3^A FW}}{d_{K_3^A 1}} = \frac{0.0315}{s^5 + 9.51s^4 + 38.35s^3 + 79.46s^2 + 79.11s + 29.67},$$

$$\frac{n_{K_3^A 2}}{d_{K_3^A 2}} = \frac{s + 3.6}{s + 0.172} \tag{61}$$

$$\frac{n_{K_3^{D-K} 1}}{d_{K_3^{D-K} 1}} = \frac{-3.3s^2 + 45.1s + 0.459}{s^2 + 0.238s + 0.0271} \cdot 10^{-4},$$

$$\frac{n_{K_3^{D-K} FW}}{d_{K_3^{D-K} 1}} = \frac{4.59 \cdot 10^{-5}}{s^2 + 0.238s + 0.0271}, \frac{n_{K_3^{D-K} 2}}{d_{K_3^{D-K} 2}} = \frac{s + 0.224}{s - 5.37 \cdot 10^{-7}} \tag{62}$$

5.4 | Comparison Study

Simulations for nominal plants of the set of plants $\tilde{\mathbf{P}}_1$, $\tilde{\mathbf{P}}_2$, $\tilde{\mathbf{P}}_3$ in the sense of Figures 4 and 5 connected in simple feedback loop (Figure 6) and 2DOF feedback loop (Figures 12a, b) are in Figures 13–18. Simulations for set of plants $\tilde{\mathbf{P}}_1$, $\tilde{\mathbf{P}}_2$, $\tilde{\mathbf{P}}_3$ perturbed by worst case perturbation (in the sense of highest upper bound μ) in Figures 19–24 show that there is no significant deterioration compared to the nominal plants. For set of plants $\tilde{\mathbf{P}}_2$ and $\tilde{\mathbf{P}}_3$ and simple feedback loop, there is an overshoot for D-K iteration disappearing for 2DOF feedback loop. The algebraic approach has an overshoot for the set of plants $\tilde{\mathbf{P}}_2$ being resolved using 2DOF feedback loop. Figures 13–24 show that algebraic approach has faster set point tracking than the D-K iteration controller.

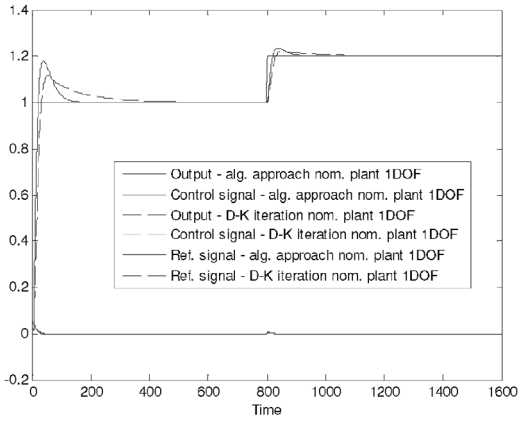

FIGURE 14 | Simulation for simple feedback loop and nominal plant of the set of plants $\tilde{\mathbf{P}}_2$.

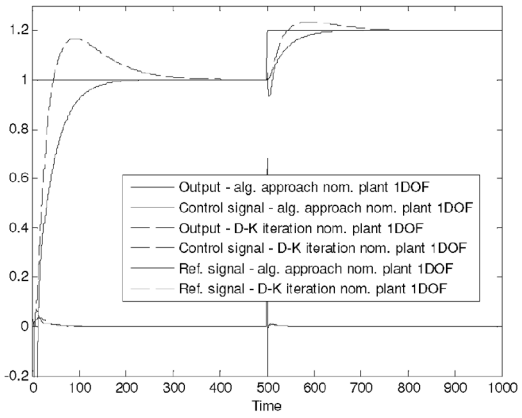

FIGURE 15 | Simulation for simple feedback loop and nominal plant of the set of plants $\tilde{\mathbf{P}}_3$.

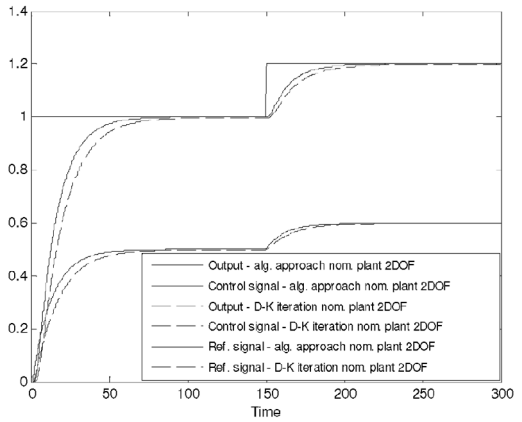

FIGURE 16 | Simulation for 2DOF feedback loop and nominal plant of the set of plants $\tilde{\mathbf{P}}_1$.

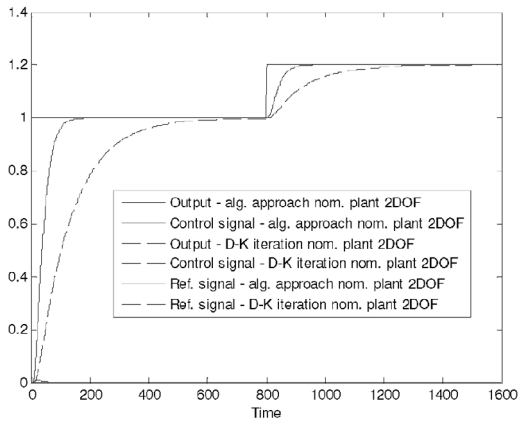

FIGURE 17 | Simulation for 2DOF feedback loop and nominal plant of the set of plants $\tilde{\mathbf{P}}_2$.

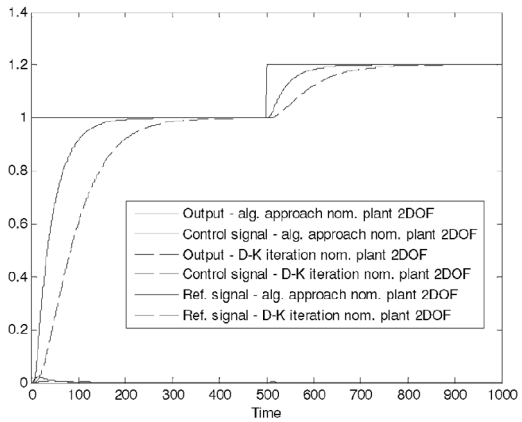

FIGURE 18 | Simulation for 2DOF feedback loop and nominal plant of the set of plants $\tilde{\mathbf{P}}_3$.

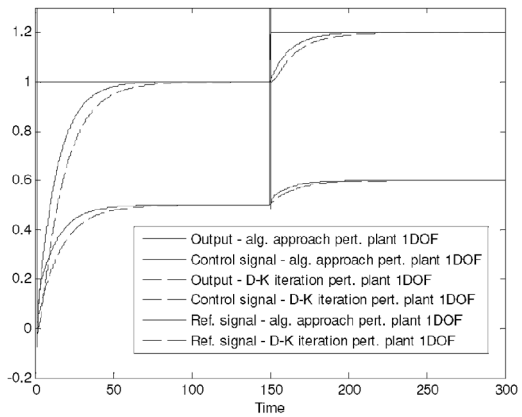

FIGURE 19 | Simulation for simple feedback loop and worst case perturbation—set of plants $\tilde{\mathbf{P}}_1$.

The simulations with set of plants $\tilde{\mathbf{P}}_1$ in Figures 13, 16, 19, and 22 prove that the D-K iteration has non-zero steady state error for both the nominal plant and plant perturbed by the worst case perturbation, unlike the controller derived via algebraic approach having zero steady state error and faster set point tracking.

Step response for set of plants $\tilde{\mathbf{P}}_1, \tilde{\mathbf{P}}_2, \tilde{\mathbf{P}}_3$ with periodic changes of their parameters are in Figures 25–27. Simulations for set of plants $\tilde{\mathbf{P}}_1, \tilde{\mathbf{P}}_2, \tilde{\mathbf{P}}_3$ with periodic changes of their parameters in Figures 28–33 demonstrate that the stability is held for both simple feedback loop and 2DOF feedback loop.

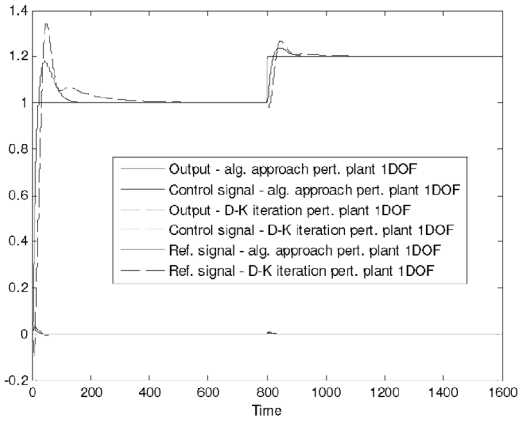

FIGURE 20 | Simulation for simple feedback loop and worst case perturbation - set of plants $\tilde{\mathbf{P}}_2$.

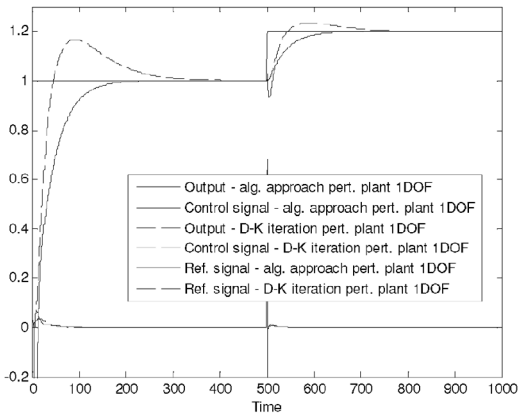

FIGURE 21 | Simulation for simple feedback loop and worst case perturbation—set of plants $\tilde{\mathbf{P}}_3$.

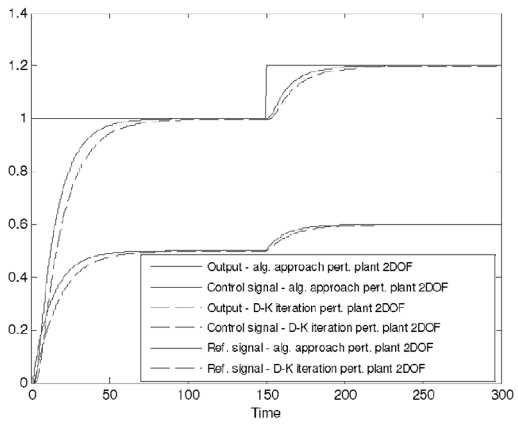

FIGURE 22 | Simulation for 2DOF feedback loop and worst case perturbation—set of plants $\tilde{\mathbf{P}}_1$.

Simulations with periodic changes of parameters were done with maximum time delays consequent upon the plant definitions (27), (34), (41), that is, $\tau_1 = \tau_2 = 4$ and $\tau_3 = 0.5$.

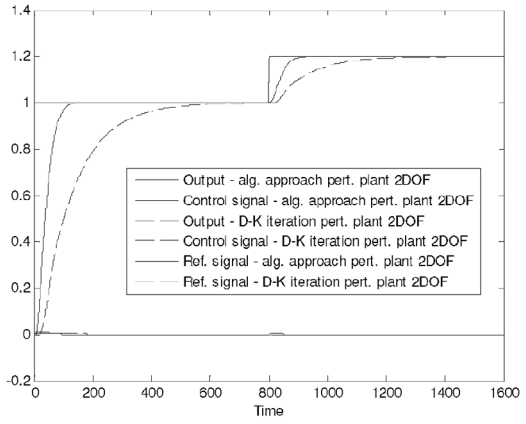

FIGURE 23 | Simulation for 2DOF feedback loop and worst case perturbation—set of plants $\tilde{\mathbf{P}}_2$.

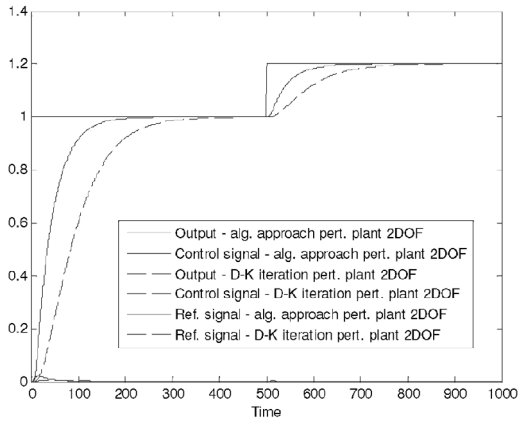

FIGURE 24 | Simulation for 2DOF feedback loop and worst case perturbation—set of plants $\tilde{\mathbf{P}}_3$.

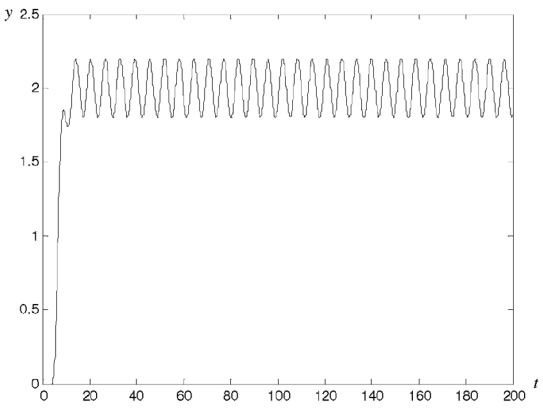

FIGURE 25 | Step response for periodic changes of parameters and set of plants $\tilde{\mathbf{P}}_1$.

6 | Conclusion

The paper demonstrated benefits of the algebraic μ-synthesis over D-K iteration as the reference method, namely the fact that the controller structure can be chosen in advance and the fact that performance weight can have astatism in its transfer function. The simulation showed that though D-K iteration acquired zero

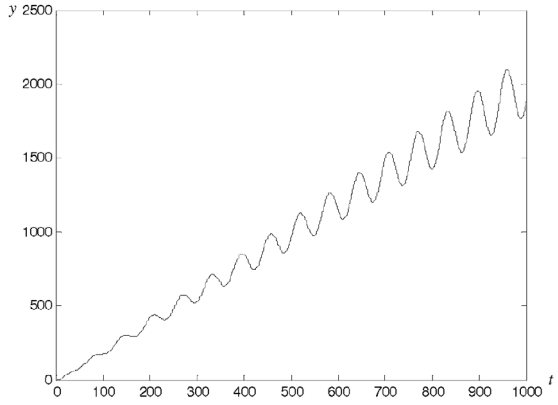

FIGURE 26 | Step response for periodic changes of parameters and set of plants $\tilde{\mathbf{P}}_2$.

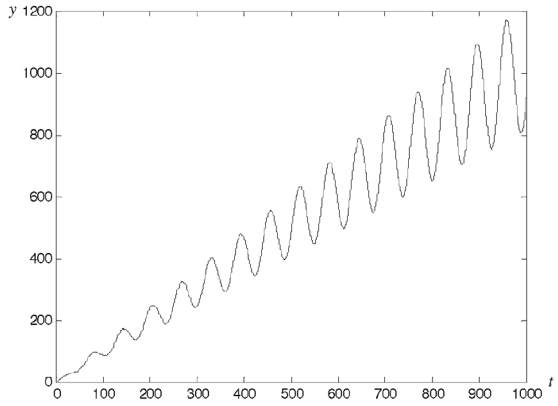

FIGURE 27 | Step response for periodic changes of parameters and set of plants $\tilde{\mathbf{P}}_3$.

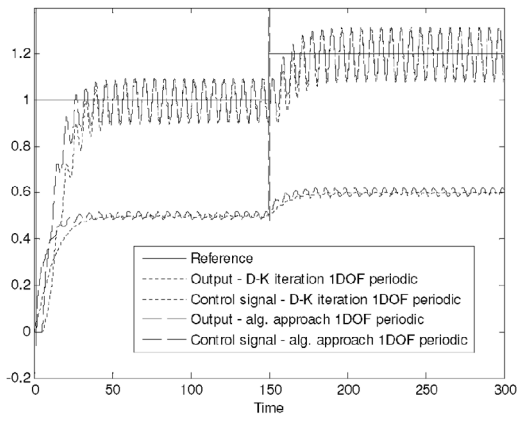

FIGURE 28 | Simulations for simple feedback loop with periodic changes—algebraic approach, D-K iteration and set of plants $\tilde{\mathbf{P}}_1$.

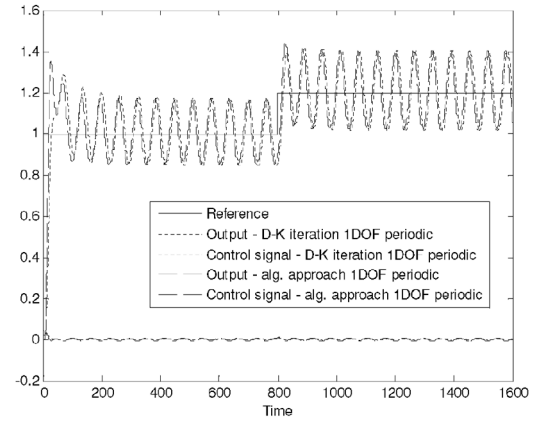

FIGURE 29 | Simulations for simple feedback loop with periodic changes—algebraic approach, D-K iteration and set of plants $\tilde{\mathbf{P}}_2$.

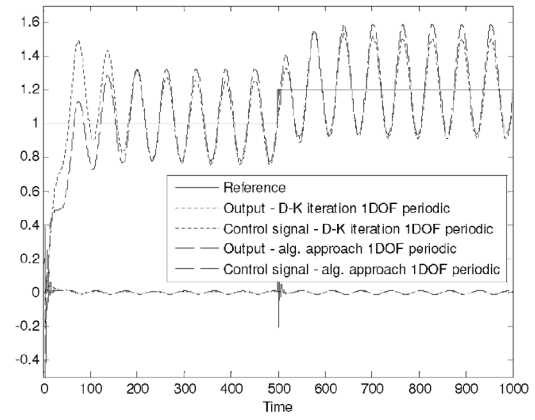

FIGURE 30 | Simulations for simple feedback loop with periodic changes—algebraic approach, D-K iteration and set of plants $\tilde{\mathbf{P}}_3$.

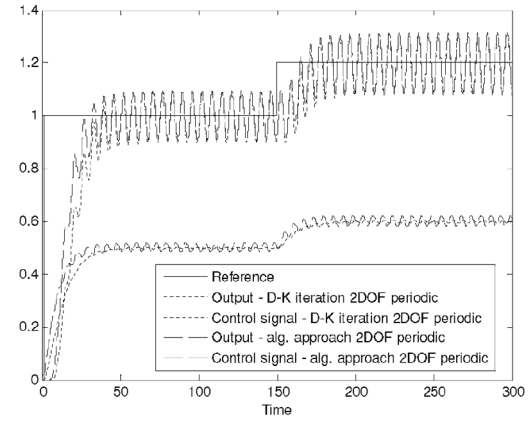

FIGURE 31 | Simulations for 2DOF feedback loop with periodic changes—algebraic approach, D-K iteration and set of plants $\tilde{\mathbf{P}}_1$.

steady state error for the controlled plants with astatism an overshoot, as drawback, appeared in time response, unlike the controller obtained using the algebraic approach.

Factorisation procedure of simple feedback loop to 2DOF interconnection for both algebraic μ-synthesis and D-K iteration has been shown and verified via simulation of step response for three plant families comprising nominal, perturbed by worst case perturbation and periodic changes case connected with 2DOF controller.

Since from the structured singular value theory follows that the stability and performance is guaranteed for the whole range of time delays, only the maximum time delay and the nominal case are studied in simulations proving functionality of both methods, that is, D-K iteration and the algebraic approach, following from

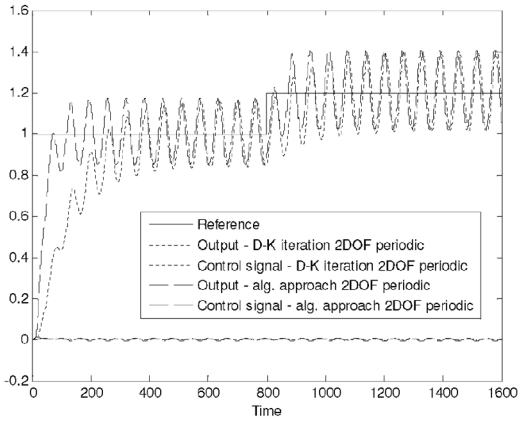

FIGURE 32 | Simulations for 2DOF feedback loop with periodic changes—algebraic approach, D-K iteration and set of plants $\tilde{\mathbf{P}}_2$.

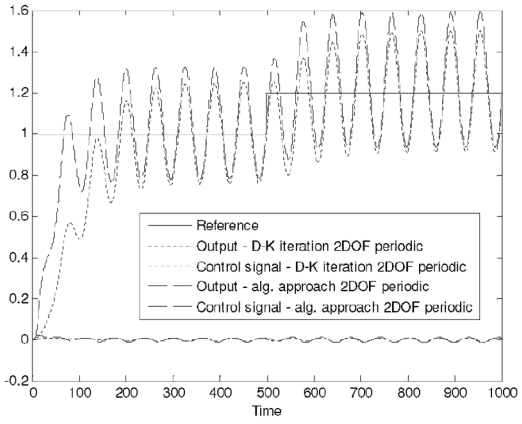

FIGURE 33 | Simulations for 2DOF feedback loop with periodic changes—algebraic approach, D-K iteration and set of plants $\tilde{\mathbf{P}}_3$.

the fact that the maximum upper bound of μ-function is lower than 1 with some margin.

The only disadvantage of the algebraic μ-synthesis is the usage of global optimisation algorithm for upper bound μ optimisation causing long time to be needed for obtaining a suitable controller and the fact that the optimality of the controller is not guaranteed. The similar issue is present in the D-K iteration causing non-optimality of the resulting D-K iteration controller consequent upon approximation of the scaling matrices D and D^{-1} by transfer function matrices $\hat{D}(s)$ and $\hat{D}^{-1}(s)$.

Author Contributions

Marek Dlapa: Conceptualisation of this study, methodology, software, writing – original draft preparation, data curation, investigation, visualisation, writing – reviewing and editing.

Acknowledgements

This work was supported by the European Regional Development Fund under the project CEBIA-Tech Instrumentation No. CZ.1.05/2.1.00/19.0376 and by the Ministry of Education, Youth and Sports of the Czech Republic within the National Sustainability Programme project No. LO1303 (MSMT-7778/2014).

Conflicts of Interest

The author declares no potential conflicts of interest.

Data Availability Statement

The article describes entirely theoretical research. Data sharing not applicable to this article as no datasets were generated or analysed during the current study.

References

1. A. Packard, and J. C. Doyle, "The Complex Structured Singular Value," *Automatica* 29, no. 1 (1993): 71–109, https://doi.org/10.1016/0005-1098(93)90175-S.

2. M. Dlapa, R. Prokop, and M. Bakošová, "Robust Control of a Two Tank System Using Algebraic Approach," in *EUROCAST 2009* (Springer, 2009), 603–609, https://doi.org/10.1007/978-3-642-04772-5_78.

3. M. Dlapa, and R. Prokop, "Algebraic Approach to Controller Design Using Structured Singular Value," *Control Engineering Practice* 18, no. 4 (2010): 358–382, https://doi.org/10.1016/j.conengprac.2009.12.005.

4. M. Dlapa, "Robust Control Design Toolbox for Time Delay Systems With Parametric Uncertainties," in *14th European Control Conference (ECC'15)* (IEEE, 2015), 788–793, https://doi.org/10.1109/ECC.2015.7330639.

5. M. Dlapa, "Differential Migration: Sensitivity Analysis and Comparison Study," in *2009 IEEE Congress on Evolutionary Computation (IEEE CEC 2009)* (IEEE, 2009), 1729–1736, https://doi.org/10.1109/CEC.2009.4983150.

6. J. C. Doyle, P. P. Khargonekar, and B. Francis, "State-Space Solutions to Standard H_2 and H_∞ Control Problems," *IEEE Transactions on Automatic Control* 34, no. 8 (1989): 358–382, https://doi.org/10.1109/9.29425.

7. P. Gahinet and P. Apkarian, "A Linear Matrix Inequality Approach to H_∞ Control," *International Journal of Robust and Nonlinear Control* 4 (1994): 421–449, https://doi.org/10.1002/rnc.4590040403.

8. K. Glover and J. C. Doyle, "State-Space Formulae for all Stabilizing Controllers That Satisfy an H_∞ Norm Bound and Relations to Risk Sensitivity," *Systems and Control Letters* 11 (1988): 167–172, https://doi.org/10.1016/0167-6911(88)90055-2.

9. G. Stein and J. C. Doyle, "Beyond Singular Values and Loopshapes," *AIAA Journal of Guidance and Control* 29, no. 1 (1991): 5–16, https://doi.org/10.2514/3.20598.

10. S. Chughtai and H. Werner, "Synthesis of Low-Order Controllers for Discrete LPV Systems Using LMIs and Evolutionary Search," in *2007 European Control Conference (ECC 2007)* (IEEE, 2007), 4861–4866, https://doi.org/10.23919/ecc.2007.7068257.

11. V. Goggos, A. Stathaki, and R. King, "Evolutionary Computation in the Design of Optimum Neural Controllers," in *European Control Conference (ECC 1999)* (1999), 49–54, https://doi.org/10.23919/ecc.1999.7098751.

12. A. Patelli and L. Ferariu, "Nonlinear System Identification by Means of Genetic Programming," in *2009 European Control Conference (ECC 2009)* (IEEE, 2009), 502–507, https://doi.org/10.23919/ecc.2009.7074452.

13. M. Dlapa, "Robust Control Design Toolbox for General Time Delay Systems via Structured Singular Value: Unstable Systems With Factorization for Two-Degree-of-Freedom Controller," in *IEEE The 22nd International Conference on Industrial Technology (IEEE ICIT 2021)* (IEEE, 2021), 93–98, https://doi.org/10.1109/ICIT46573.2021.9453505.

14. J. C. Doyle, "Structure Uncertainty in Control System Design," in *24th IEEE Conference on decision and control* (1985): 260–265, https://doi.org/10.1109/cdc.1985.268842.

15. J. C. Doyle, J. Wall, and G. Stein, "Performance and Robustness Analysis for Structured Uncertainty," in *21st IEEE Conference on Decision and Control* (IEEE, 1982), 629–636, https://doi.org/10.1109/cdc.1982.268218.